photonics

MDPI

Communication

Improving the Performance of Optical Phased Array by Reducing Relative Intensity Noise of Optically Injection-Locked Laser Array

Anh-Hang Nguyen [1] and Hyuk-Kee Sung [2,*]

[1] Department of Electronic and Electrical Engineering, Hongik University, Seoul 04066, Republic of Korea
[2] School of Electronic and Electrical Engineering, Hongik University, Seoul 04066, Republic of Korea
* Correspondence: hksung@hongik.ac.kr

Abstract: Relative intensity noise (RIN) is an important factor that determines the performance of optical phased arrays (OPA) that are configured using semiconductor lasers as light emission sources. This study proposes a method of improving the optical signal-to-noise ratio (OSNR) of an OPA by reducing the RIN and using high coherence of optically injection-locked (OIL) laser arrays. We numerically demonstrated a laser RIN reduction of 22.7 dB by the OIL laser compared to a free-running laser. We achieved an OPA RIN reduction of 13.2 dB by combining the coherent outputs with the uncorrelated noise of 21 OIL lasers, compared to a single OIL laser RIN. Consequently, we demonstrated an OPA OSNR increase of approximately 13.8 dB based on the OIL-based OPA compared to that of the conventional noise-correlated OPA configuration. Additionally, we confirmed the maintenance of OPA OSNR improvement during OPA operations.

Keywords: optical injection locking; laser relative intensity noise; optical phased array; optical signal-to-noise ratio

Citation: Nguyen, A.-H.; Sung, H.-K. Improving the Performance of Optical Phased Array by Reducing Relative Intensity Noise of Optically Injection-Locked Laser Array. *Photonics* **2022**, *9*, 868. https://doi.org/10.3390/photonics9110868

Received: 18 October 2022
Accepted: 16 November 2022
Published: 17 November 2022

1. Introduction

Optical phased array (OPA), a nonmechanical beam steering technology based on the coherence of optical signals [1], has been widely studied and employed in several applications such as optical wireless communications (OWC) [2], light detection and ranging (LiDAR) [3], and optical imaging [4] owing to its notable advantages, such as low cost, small form-factor, low power consumption, and scalable output power [1]. Various approaches, such as the use of passive optical waveguides fed by an optical source [1], optical phased locked loops [5], and injection-locked lasers [6,7], have been implemented to obtain coherence between optical emitters to achieve high-performance OPA systems. OPA configured using optically injection-locked (OIL) lasers are considered promising candidates owing to their compactness, low loss, and low power consumption [1,7].

Lasers are essential elements in OPA owing to their properties, such as coherence, monochromaticity, and directionality, which enable a narrow and steerable OPA beam with high resolution [1,8]. However, the laser intensity noise, which fluctuates around the steady state value of the laser output power, is a considerable issue because of its limitation on the precision and reliability of OPA applications [9,10]. The intensity noise is characterized by the relative intensity noise (RIN), which is defined as the ratio of the noise spectral density to the laser average power [8]. Furthermore, precision and reliability are determined by the optical signal-to-noise ratio (OSNR), which is defined as the ratio of the noise power to the OPA signal power [8,9]. Therefore, a laser RIN reduction is required to enhance the OSNR of the OPA system.

Studies have reported various laser RIN reduction methods, such as increasing the laser power [11], optoelectronic feedback [12], and OIL lasers [13]. The RIN of an OIL laser can be further reduced by a factor of approximately 1/N by configuring an N-element

array of OIL lasers [14]. We previously reported an OPA system using an OIL laser array based on the strong coherence property and simultaneous amplitude (AM) and phase (PM) modulation of the OIL laser to achieve sidelobe reduction and beam steering of the OPA system [7]. The OIL-based OPA system was configured using a master laser (ML) and an array of slave lasers (SLs). The coherence and stability of the optical output signals are obtained owing to the optical injection of ML into the SL array within the stable-locking condition [15,16]. Consequently, RIN reduction of the OIL laser array used for the OPA system can be achieved to enhance the OSNR and improve the OIL-based OPA performance.

In this study, we theoretically investigate the OSNR enhancement of OPA signals based on RIN reduction using an OIL laser array. First, we introduced the principle to improve the OSNR of the OIL-based OPA based on the RIN reduction of the OIL laser array by presenting the concept of an OPA configuration with high-coherence and low-RIN output signals based on an OIL laser array. Second, we numerically demonstrated a 22.7 dB reduction in the laser RIN of a single OIL laser compared to a free-running laser. Then, we simulated the combination of coherent signals with uncorrelated noises generated by an array of OIL lasers and achieve a reduction of 13.2 dB in OPA RIN compared to a single OIL laser RIN. Consequently, we achieved an improvement of 13.8 dB OSNR using 21 OIL laser emitters compared to a noise-correlated OPA configuration. Finally, we confirm that the enhanced OSNR and reduced sidelobe level of the OIL-based OPA can be sustained during beam steering.

2. Principle to Improve Optical Signal-to-Noise Ratio of OIL-Based OPA

Figure 1 shows a schematic of the OPA configured by an ML and N-element array of SLs, whereas a single OIL laser configuration comprises an ML and an SL [7]. When the OIL laser parameters between the ML and SL are properly controlled, the OIL laser exhibits significant performance improvements such as improved frequency stability, low chirping, resonance frequency increase, high coherence, and RIN reduction [13,15–17].

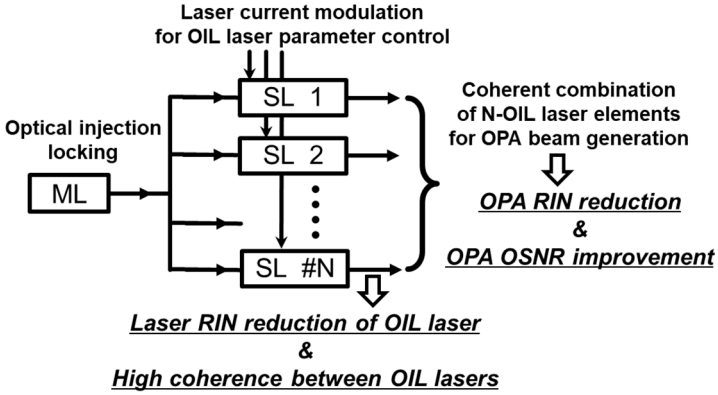

Figure 1. Schematic of optical phased array (OPA) configured by a master laser and N-optically injection-locked (OIL) semiconductor lasers to achieve laser relative intensity (RIN) reduction, high coherence, OPA RIN reduction, and OPA optical signal-to-noise ratio (OSNR) improvement. ML: master laser, SL: slave laser.

The two OIL laser parameters are the injection ratio ($R = S_{inj}/S_{free,SL}$) and detuning frequency ($\Delta f = f_{ML} - f_{free,\,SL}$). We define S_{inj}, $S_{free,SL}$, f_{ML}, and $f_{free,\,SL}$ as the injection photon numbers from the ML to the SL cavity, photon numbers of the free-running SL, lasing frequency of the ML, and lasing frequency of the free-running SL, respectively. By varying the OIL laser parameters within a stable locking regime, we achieved AM and PM of the OIL laser along with significant laser performance improvements. Optical AM and PM are essential for OPA beam steering and sidelobe reduction [7]. The modulation of the bias current in the SL enables the simultaneous control of the OIL laser parameters [7,13,18].

In this study, we propose RIN reduction and OSNR improvement of OPA signals based on OIL-based OPA. As shown in Figure 1, OIL laser elements were used as OPA emitters in the OIL-based OPA. An SL element can exhibit a low laser RIN and high coherent beam quality owing to the OIL effect. Moreover, the OPA signal generated by N-OIL laser elements can exhibit a much lower RIN owing to the coherent combination effect of uncorrelated noise OIL signals [14]. Therefore, the OPA OSNR can be enhanced to improve OPA performance using the proposed OIL-based OPA.

3. Simulation Results

The RIN reduction achievement of the OIL laser is calculated based on the rate-equation model, including the spontaneous emission rate and the Langevin noise sources, which are ignored in ideal cases [13]. The OIL rate equations with noise sources are expressed as:

$$\frac{dS(t)}{dt} = \{g[N(t) - N_{tr}] - \gamma_p\}S(t) + 2\kappa\sqrt{S_{inj}S(t)}\cos(\phi(t)) + \beta R_{sp} + F_S(t), \quad (1)$$

$$\frac{d\phi(t)}{dt} = \frac{\alpha}{2}\{g[N(t) - N_{tr}] - \gamma_p\} - 2\kappa\sqrt{S_{inj}S(t)}\sin(\phi(t)) + -2\pi\Delta f + F_\phi(t), \quad (2)$$

$$\frac{dN(t)}{dt} = J_{bias} - \gamma_n N(t) - g[N(t) - N_{tr}]S(t) - R_{sp} - R_{nr} + F_N(t), \quad (3)$$

$$P(t) = \frac{hc\eta\gamma_p}{\lambda}S(t), \quad (4)$$

where $S(t)$, $\phi(t)$, $N(t)$, and $P(t)$ are the photon number, field phase, carrier number, and laser output power, respectively. g is the linear gain, N_{tr} is the transparency carrier number, β is the spontaneous emission factor, R_{sp} is the spontaneous emission rate, R_{nr} is the nonradiative recombination rate, γ_p is the photon decay rate, γ_n is the carrier decay rate, h is Planck's constant, and η is the quantum efficiency. The coupling rate κ, injected photon number S_{inj}, and the detuning frequency Δf are the OIL terms. $F_S(t)$, $F_\phi(t)$, and $F_N(t)$ are the photon, phase, and carrier Langevin noise sources, and are expressed as [19]:

$$F_S(t) = \sqrt{\frac{2\beta S(t)N(t)\gamma_n}{\Delta t}}x_S, \quad (5)$$

$$F_\phi(t) = \sqrt{\frac{\beta N(t)\gamma_n}{2S(t)\Delta t}}x_\phi, \quad (6)$$

$$F_N(t) = \sqrt{\frac{2N(t)\gamma_n(1 + \beta S(t))}{\Delta t}}x_N, \quad (7)$$

where x_S, x_ϕ, and x_N are independent random numbers with Gaussian distributions of zero means and variances of unity, and Δt is the sampling time interval.

The output power of the laser with noise is expressed as $P(t) = P_0 + \delta P(t)$, where P_0 is the time average power and $\delta P(t)$ is the optical power fluctuation. To measure and quantify the intensity noise, RIN was introduced and can be expressed as [8]:

$$RIN = \frac{\left\langle \delta P(t)^2 \right\rangle}{P_0^2}, \quad (8)$$

where $\left\langle \delta P(t)^2 \right\rangle$ is the mean square time-averaged power fluctuation. In the frequency domain, RIN is redefined as:

$$RIN = \frac{2S_{\delta P}(f)}{P_0^2\Delta F}, \quad (9)$$

where $S_{\delta P}(\omega)$ is the noise spectral density of $\delta P(t)$ at the frequency f and ΔF is the measurement bandwidth.

Figure 2 shows the RIN of the free-running laser (black), OIL laser (blue), and the OPA signal (red) with 21 elements of the OIL laser array. To simulate the laser RIN, we use ordinary differential equation (ODE) solver in MATLAB, obtain time-domain solution of laser output power, and execute a fast Fourier transform (FFT) for the laser output power. The physical parameters of the master and slave lasers used in our simulation are presented in [13]. As shown in Figure 2, the RIN of the free-running laser exhibited the highest peak of −133.3 dB/Hz, which corresponded to its relaxation oscillation frequency of 4.8 GHz. The OIL laser operating under OIL laser parameters of R = 5 dB and $\Delta f = -5$ GHz exhibited a higher resonant frequency (22.7 GHz) and RIN reduction (22.7 dB) compared to the free-running laser. It was reported that the resonant frequency and RIN performance of the OIL laser were functions of the OIL laser parameters, and the improvement over free-running lasers was maintained throughout the entire stable locking range [13]. Next, we combined the outputs of the N-element OIL laser array to produce the OPA signal (N = 21). The RIN of the combined optical signal, called OPA RIN, was reduced by 13.2 dB, compared to the single OIL laser RIN, owing to the signal noise suppression caused by the summation of highly coherent signals with uncorrelated noise [14]. Because we employed a coherent 21-OIL laser array, we confirmed that the 13.2 dB reduction corresponded to a 21 times reduction in the linear scale. It should be noted that the coherence between all OIL laser arrays in our proposed OPA schematic was due to the phase-locking effect achieved by laser injection locking. Consequently, we concluded that the combination of highly coherent signals with low-RIN emitters can significantly improve the OPA RIN performance, as shown in the red plot in Figure 2.

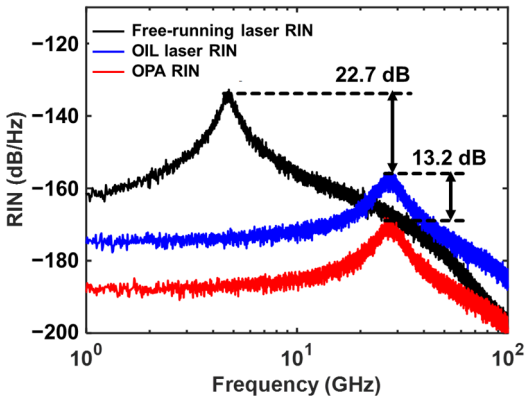

Figure 2. RIN of free-running laser (black), OIL laser (blue), and OPA with 21-element array (red).

Figure 3 shows a passive-waveguide OPA schematic configured by a single OIL laser source and an array of passive optical waveguides. Although a free-running laser is typically used as an optical source for the passive-waveguide type of OPA configuration, we replace it with a single OIL laser. This is to compare the effect of the single OIL laser and arrayed OIL lasers. The OIL laser exhibits advantages over the free-running laser such as the frequency stability as well as RIN reduction [13]. In the passive-waveguide OPA configuration, a single OIL laser is followed by an optical splitter and passive optical waveguides used as the OPA emitters. Beam steering is achieved using phase modulators in the waveguides. The output optical signals emitted from the passive waveguides exhibit the correlated noise because they are distributed from an optical source signal. The OPA signal generated by combining coherent signals with correlated noise exhibit an increase in both the signal and noise powers. In contrast, the proposed OIL-based OPA (Figure 1) exhibits highly coherent output optical signals with low noise because the noise of each element is uncorrelated. Therefore, the RIN of the OPA signal using N-slave lasers is reduced owing to the coherent combination of the signal beams and the incoherent combination of the noise beams. Therefore, the OSNR of the proposed OIL-based OPA signal is enhanced. To

verify the enhancement of the OSNR performance, we compare the OSNRs of the proposed OIL-based OPA configured by OIL laser array (Figure 1) and the passive-waveguide OPA configured by a single OIL laser and passive optical waveguide array (Figure 3).

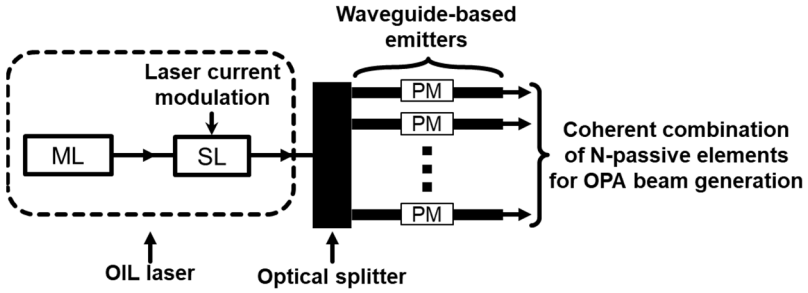

Figure 3. Schematic of the passive-waveguide optical phased array (OPA) configured by a single optically injection-locked (OIL) semiconductor laser and N passive optical waveguides. ML: master laser, SL: slave laser, PM: phase modulator.

Figure 4 shows the simulation results for the OSNR improvement of the OPA system based on the OIL laser array. The OSNR of the 21-element OPA using the OIL laser array (red color, Figure 1) and passive waveguide array (blue color, Figure 3) was calculated using the laser parameters in [13]. The 21 OIL laser elements were operated within the same locking conditions to maintain a high sidelobe level of −13 dB at 0°, as shown in the inset of Figure 4. The resonant frequencies of both OPA systems were set at 27.5 GHz for a fair comparison. The OIL-based OPA (N-slave lasers) exhibited a 13.8 dB increase in OSNR compared to that of the passive-waveguide OPA (single OIL laser) throughout the entire frequency range.

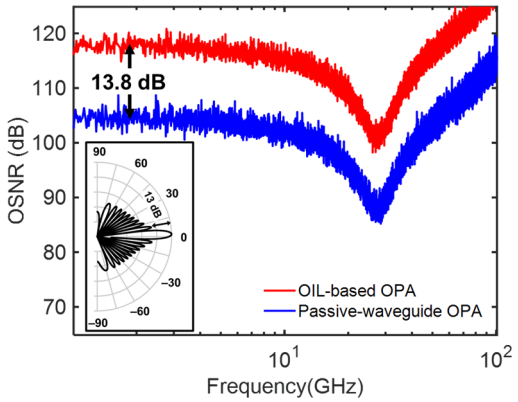

Figure 4. Comparison of OPA OSNR ((N = 21) based on OIL laser elements (red) and noise-correlated passive waveguides (blue), respectively. Inset: OPA pattern with −13 dB of sidelobe level.

Finally, we confirmed the improvement in the OSNR with a low sidelobe level during beam steering. Note that beam steering and sidelobe reduction can be achieved by varying the two OIL laser parameters in a stable locking regime [7]. Figure 5a shows the assignment of injection-locking parameters to the 21 OIL lasers to achieve beam steering of 0° (black crosses) and 2° (red crosses) with a low sidelobe level of −30 dB. The appropriate assignment of the OIL parameters to the OIL-based OPA elements can be calculated based on the locking map, as reported in [7]. Figure 5b represents the corresponding OSNR performances of OIL-based OPA of beam steering at 0° (black) and 2° (red) with SLL of −30 dB. We confirmed that high OSNR performance was maintained at the same level at different beam-steering angles. The inset of Figure 5b shows the far-field radiation pattern of the OPA with a low sidelobe level of −30 dB for beam steering angles of 0° (dotted line) and 2° (solid line).

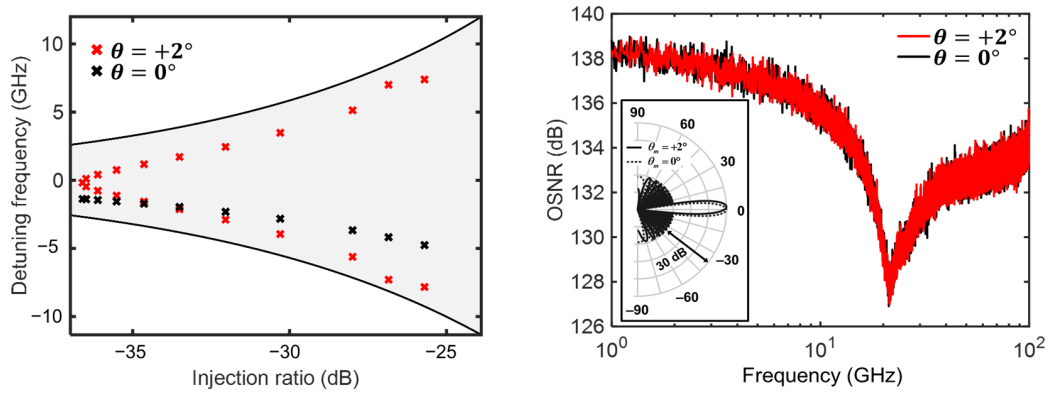

(**a**) (**b**)

Figure 5. (**a**) The injection-locking parameter assignment in the locking map for 21 OIL lasers to achieve beam steering of 0° (black crosses) and 2° (red crosses) with a sidelobe level of −30 dB. (**b**) The OSNRs of OIL-based OPA during steering at 0° (black) and 2° (red) directions. Inset: Far-field OPA pattern during beam steering with a low sidelobe level of −30 dB.

4. Conclusions

In this study, we enhanced the OSNR of the OPA configuration using an OIL laser array based on RIN reduction. The optical signal of the OIL laser element exhibited a low RIN with high coherence. By combining the optical beams of the OIL laser elements, we achieved an OPA signal with low RIN and high OSNR. First, we calculated the RIN of each OIL laser element and confirmed a laser RIN reduction of 22.7 dB compared to a free-running laser. Second, we theoretically achieved a 13.2 dB RIN reduction (compared to a single-laser RIN) and a 13.8 dB OSNR increase (compared to a noise-correlated OPA configuration) by OIL-based OPA (N = 21). Moreover, the enhanced OSNR performance and low sidelobe level of the OIL-based OPA were simultaneously achieved and maintained during beam steering to ensure the OPA performance throughout its operation. We believe that the OIL-based OPA with high power, low sidelobe levels, and high OSNR can be widely applied in various optical and radio frequency (RF) applications, such as reliable optical sensors, long-range LiDAR, and high speed optical/RF wireless communication.

Author Contributions: For research articles with several authors, a short paragraph specifying their individual contributions is required. The following statements were used: Conceptualization, A.-H.N. and H.-K.S.; simulation, A.-H.N.; analysis, A.-H.N. and H.-K.S.; writing—original draft preparation, A.-H.N.; writing—review and editing, H.-K.S.; visualization, H.-K.S.; supervision, H.-K.S. All authors have read and agreed to the published version of the manuscript.

Funding: This work was funded by the National Research Foundation of Korea (NRF) under the Basic Science Research Program (NRF-2019R1F1A1040959 and NRF-2021R1F1A1045919).

Institutional Review Board Statement: Not applicable.

Informed Consent Statement: Not applicable.

Data Availability Statement: Not applicable.

Conflicts of Interest: The authors declare no conflict of interest. The funders had no role in the study design, collection, analyses, or interpretation of data, in the writing of the manuscript, or in the decision to publish the results.

References

1. Heck, M.J.R. Highly integrated optical phased arrays: Photonic integrated circuits for optical beam shaping and beam steering. *Nanophotonics* **2017**, *6*, 93–107. [CrossRef]
2. Wang, L.; Nirmalathas, A.; Lim, C.; Wong, E.; Alameh, K.; Li, H.; Skafidas, E. High-speed indoor optical wireless communication system employing a silicon integrated photonic circuit. *Opt. Lett.* **2018**, *43*, 3132–3135. [CrossRef] [PubMed]

3. Hsu, C.-P.; Li, B.; Solano-Rivas, B.; Gohil, A.R.; Chan, P.H.; Moore, A.D.; Donzella, V. A Review and Perspective on Optical Phased Array for Automotive LiDAR. *IEEE J. Sel. Top. Quantum Electron.* **2021**, *27*, 8300416. [CrossRef]
4. Aflatouni, F.; Abiri, B.; Hajimiri, A. Nanophotonic projection system. *Opt. Express* **2015**, *23*, 21012–21022. [CrossRef] [PubMed]
5. Vilenchik, Y.; Erkmen, B.I.; Satyan, N.; Yariv, A.; Farr, W.H.; Choi, J.M. Optical phase lock loop based phased array transmitter for optical communications. *Interplanet. Netw. Prog. Rep.* **2011**, *42-184*, 1–17.
6. Sayyah, K.; Efimov, O.; Patterson, P.; Schaffner, J.; Xu, G.; Miglo, A. Two-dimensional pseudo-random optical phased array based on tandem optical injection locking of vertical cavity surface emitting laser. *Opt. Express* **2015**, *23*, 19405–19416. [CrossRef]
7. Nguyen, A.-H.; Cho, J.-H.; Sung, H.-K. Side-lobe Level Reduction of an Optical Phased Array Using Amplitude and Phase Modulation of Array Elements Based on Optically Injection-Locked Semiconductor Lasers. *Photonics* **2020**, *7*, 20. [CrossRef]
8. Coldren, L.A.; Corzine, S.W.; Mašanović, M.L. *Diode Lasers and Photonic Integrated Circuits*, 4th ed.; John Wiley & Sons: Hoboken, NJ, USA, 2012; pp. 257–275.
9. Yang, C.; Xu, S.; Qi, Y.; Mo, S.; Li, C.; He, X.; Feng, Z.; Yang, Z.; Jiang, Z. High OSNR watt-level single-frequency one-stage PM-MOPA fiber laser at 1083 nm. *Opt. Express* **2014**, *22*, 1181–1186. [CrossRef] [PubMed]
10. Binh, L.N. *Optical Fiber Communication Systems with MATLAB and Simulink Models*, 2nd ed.; CRC Press: Florida, FL, USA, 2015; pp. 103–145.
11. Faugeron, M.; Tran, M.; Parillaud, O.; Chtioui, M.; Robert, Y.; Vinet, E.; Enard, A.; Jacquet, J.; Van Dijk, F. High-Power Tunable Dilute Mode DFB Laser with Low RIN and Narrow Linewidth. *IEEE Photonics Technol. Lett.* **2013**, *25*, 7–10. [CrossRef]
12. Zhao, Q.; Xu, S.; Zhou, K.; Yang, C.; Li, C.; Feng, Z.; Peng, M.; Deng, H.; Yang, Z. Broad-bandwidth Near-Shot-Noise-Limited Intensity Noise Suppression of A Single-Frequency Fiber laser. *Opt. Lett.* **2016**, *41*, 1333–1335. [CrossRef] [PubMed]
13. Lau, E.K.; Wong, J.; Wu, M.C. Enhanced Modulation Characteristics of Optical Injection-Locked Lasers: A Tutorial. *IEEE J. Sel. Top. Quantum Electron.* **2009**, *15*, 628–633. [CrossRef]
14. She, X.; Xiong, B.; Sun, C.; Hao, Z.; Wang, J.; Wang, L.; Han, Y.; Li, H.; Luo, Y. Coherently Combined DFB Laser Array Chip with Reduced Relative Intensity Noise. *IEEE Photonics Technol. Lett.* **2021**, *33*, 986–989. [CrossRef]
15. Sung, H.-K.; Lau, E.K.; Wu, C.M. Optical Properties and Modulation Characteristics of Ultra-Strong Injection-Locked Distributed Feedback Lasers. *IEEE J. Sel. Top. Quantum Electron.* **2007**, *13*, 1215–1221. [CrossRef]
16. Liu, Z.; Slavík, R. Optical Injection Locking: From Principle to Applications. *J. Light. Technol.* **2020**, *38*, 43–59. [CrossRef]
17. Nazarikov, G.; Rommel, S.; Yao, W.; Tafur Monroy, I. Optical Injection Locking for Generation of Tunable Low-Noise Millimeter Wave and THz Signals. *Appl. Sci.* **2021**, *11*, 10185. [CrossRef]
18. Lee, H.; Cho, J.H.; Sung, H.K. Theoretical Analysis of a Method for Extracting the Phase of a Phase-Amplitude Modulated Signal Generated by A Direct-Modulated Optical Injection-Locked Semiconductor Laser. *Opt. Eng.* **2017**, *56*, 056112. [CrossRef]
19. Fatadin, I.; Ives, D.; Wicks, M. Numerical Simulation of Intensity and Phase Noise from Extracted Parameters for CW DFB Lasers. *IEEE J. Quantum Electron.* **2006**, *42*, 934–941. [CrossRef]